Available online at www.sciencedirect.com
ScienceDirect
Trans. Nonferrous Met. Soc. China 24(2014) 2003−2017
Transactions of Nonferrous Metals Society of China
www.tnmsc.cn

Heat treatment of 7xxx series aluminium alloys—Some recent developments

Paul A. ROMETSCH, Yong ZHANG, Steven KNIGHT

Department of Materials Engineering, Monash University, Wellington Road, Clayton, VIC 3800, Australia

Received 17 October 2013; accepted 10 April 2014

Abstract: The 7xxx series alloys are heat treatable wrought aluminium alloys based on the Al−Zn−Mg(−Cu) system. They are widely used in high-performance structural aerospace and transportation applications. Apart from compositional, casting and thermo-mechanical processing effects, the balance of properties is also significantly influenced by the way in which the materials are heat-treated. This paper describes the effects of homogenisation, solution treatment, quenching and ageing treatments on the evolution of the microstructure and properties of some important medium to high-strength 7xxx alloys. With a focus on recent work at Monash University, where the whole processing route from homogenisation to final ageing has been studied for thick plate products, it is reported how microstructural features such as dispersoids, coarse constituent particles, fine-scale precipitates, grain structure and grain boundary characteristics can be controlled by heat treatment to achieve improved microstructure−property combinations. In particular, the paper presents methods for dissolving unwanted coarse constituent particles by controlled high-temperature treatments, quench sensitivity evaluations based on a systematic study of continuous cooling precipitation behaviour, and ageing investigations of one-, two- and three-step ageing treatments using experimental and modelling approaches. In each case, the effects on both the microstructure and the resulting properties are discussed.

Key words: 7xxx aluminium alloys; Al−Zn−Mg−Cu; homogenisation; solution treatment; quenching; retrogression and re-ageing; strength; corrosion

1 Introduction

High-strength age-hardened 7xxx series Al−Zn−Mg−Cu alloys are widely used for aircraft structures, where they are subjected to demanding operating conditions. Important properties that must be considered for these applications are strength, ductility, modulus, corrosion and damage tolerance (e.g. fracture toughness and fatigue resistance). Most of these properties can be controlled through appropriate alloying, processing or a combination of these. Age-hardenable 7xxx series aluminium alloys for high-performance structural applications are typically processed in the form of plates, extrusions or forgings. For thick plate products, a typical processing schedule involves casting, homogenising, hot rolling, solution treating, quenching, stress relieving by stretching and age hardening, as shown in Fig. 1.

The focus of this paper is on some of the recent metallurgical developments related especially to the heat treatment processes of homogenisation, solution treatment, quenching and ageing. This paper describes some important effects of these heat treatment processes on the evolution of the microstructure and properties of some important medium to high-strength 7xxx series alloys. Focused around work carried out at Monash University from about 2005 to 2013, the paper describes how metallurgical features such as Al_3Zr dispersoids, coarse constituent particles (e.g. Al_2CuMg, $MgZn_2$, Mg_2Si and Al_7Cu_2Fe), fine-scale precipitates (e.g. η'), the grain structure and grain boundary characteristics can be controlled to achieve desirable microstructure−property combinations. It is important to note that the whole processing route from homogenisation to final ageing has been investigated on commercial materials in significant detail. This is valuable since most studies focus either only on experimental lab-scale materials or just on the beginning or end of the processing route due to difficulties in obtaining commercial materials from intermediate processing stages. In particular, the paper presents findings about 1) the dissolution of unwanted coarse constituent particles by means of controlled high-temperature heat treatments, 2) the quench sensitivity investigated under continuous cooling conditions, and 3) the ageing behaviour during one-, two- and three-step ageing treatments, including retrogression and re-ageing

Corresponding author: Paul A. ROMETSCH; Tel: +61-3-99053655; E-mail: paul.rometsch@monash.edu
DOI: 10.1016/S1003-6326(14)63306-9

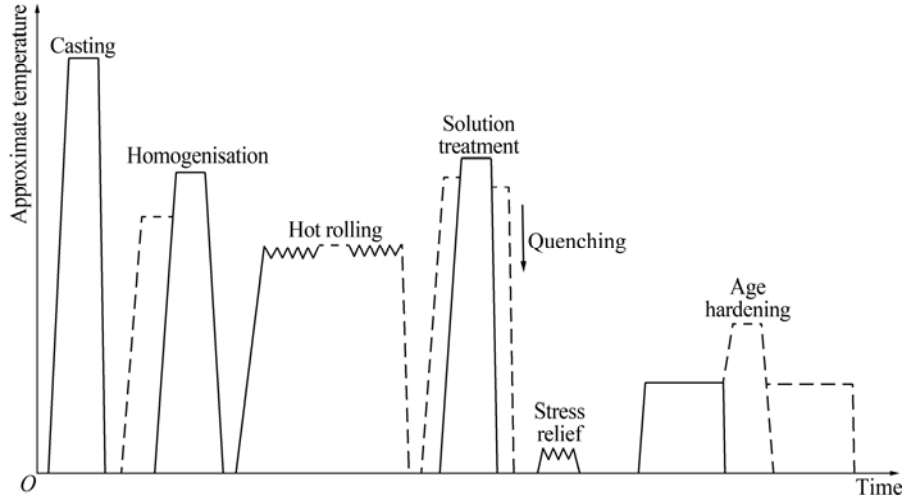

Fig. 1 Semi-schematic processing schedule for high-strength Al−Zn−Mg−Cu plate (Some commercial and experimental variations are indicated by dashed lines)

(RRA). In each case, the effects on both the microstructure and the resulting properties are discussed.

In order to set this discussion into the broader context of the whole processing schedule shown in Fig. 1, some general introductory comments will first be made about casting, homogenisation and hot rolling. Although hot rolling could here be substituted by extrusion or forging (either with or without subsequent solution treatment), for simplicity and clarity only hot rolling is discussed here.

Casting: When the aluminium alloy is cast, the most rapid cooling and solidification occurs near the surfaces of the casting. Dendrites of the aluminium-rich α-phase grow in the direction of the temperature flow, resulting in compositional differences on both the macro (cm to m) and micro-scales (< mm). Micro-segregation may be removed by a suitable homogenisation treatment. Macro-segregation occurs on a scale where subsequent annealing heat treatments are unable to redistribute the solute, and can lead to material having localised areas outside the nominal specifications. The solidification process also produces equilibrium or metastable constituent phases that are formed by a liquid-solid eutectic reaction [1]. These coarse particles are often insoluble in the solid state after casting, incoherent with the matrix, and normally form interdendritically. A variety of constituent particles have been identified in 7xxx series Al alloys, such as the Fe- or Si-containing Al_7Cu_2Fe and Mg_2Si phases. Copper contents are usually limited in 7xxx series alloys to curtail the formation of large intermetallic particles, such as *S*-phase (Al_2CuMg). Modelling shows that this compound is formed at mass fractions of Cu+Mg ≥3.6% in 7xxx alloys containing around 6% Zn [2]. The volume fraction of constituent particles is normally 1%−5%, while their sizes range from about 5 to 30 μm, depending on processing conditions [3]. The presence of relatively large constituent particles can be detrimental to the strength, fatigue resistance, and fracture toughness of the alloy. Therefore, most modern high-strength Al alloys have low Fe and Si contents in order to improve the mechanical properties [4].

Homogenisation: Homogenisation is typically carried out at 450−500 °C, but temperatures can vary widely depending on the alloy composition. One of the main purposes is to reduce the micro-scale segregation formed during casting. In 7xxx series alloys, alloying elements such as Cr, Mn and Zr form dispersoid particles during homogenisation, which have the effect of reducing grain growth and inhibiting recrystallisation during subsequent high-temperature processing. In 7xxx series alloys, dispersoids account for volume fractions of about 0.05%−0.2%, with typical particle sizes ranging from about 20 to 500 nm [3]. Dispersoid phases such as $Al_{18}Mg_3Cr_2$ or $Al_{12}Mg_2Cr$ (size: 50−300 nm) may form in Cr-containing alloys [5,6], the Al_3Zr phase (size: 20−60 nm) in Zr-containing alloys [5,6], and both Al_6Mn and $Mn_3Si_2Al_{15}$ have been reported in Mn-containing alloys [7]. Dispersoids containing Cr or Mn are generally incoherent with the matrix, while Zr-containing dispersoids may be coherent with the matrix [8]. There is a gradual increase in the fracture toughness of alloys with a particular composition when the dispersoid type changes from predominantly Mn-based, to Cr-based, to Zr-based. This increase in fracture toughness may stem from a decrease in the average dispersoid size, although other factors such as the increasing modulus of the dispersoid phase, and differences in dispersoid particle cohere all compound and complicate the actual effects of dispersoid type on

fracture toughness [3].

In modern high-performance alloys, Al_3Zr is the preferred dispersoid due to its improved ability to inhibit recrystallisation (which can also increase the toughness) without significantly increasing the quench sensitivity. It has been demonstrated for alloys AA7050 and AA7150 that an improved size distribution of $L1_2$ Al_3Zr dispersoids and recrystallisation inhibition effect may be obtained by performing two-step homogenisation treatments aiming at first stimulating nucleation at <440 °C and subsequently promoting controlled growth at >450 °C [9−11]. The higher temperature step may also be used to dissolve coarse $MgZn_2$ or Al_2CuMg constituents, although these may re-precipitate during slow cooling and promote particle-stimulated nucleation (PSN) of recrystallisation during subsequent solution treatment [12]. In this respect, a relatively fast cooling rate from a high-temperature homogenisation treatment has been demonstrated to decrease both the particle size and the final recrystallised fraction [12,13]. In cases where the required fast cooling rates are not practically achievable for large rolling slabs, similar improvements may be achieved by performing the homogenisation treatment as a preheating treatment just before hot rolling [12]. This could also translate into overall improvements in productivity and energy consumption.

Hot rolling: During hot rolling, ingots up to 1 m in thickness are reduced to 50−150 mm in thickness using multiple passes at ~ 400 °C. The grain structure develops an elongated pancake-type morphology as a result of the rolling. Constituent particles are broken up and dispersed in the direction of rolling (stringers). Significant dynamic recovery usually occurs during hot rolling, whereby dislocations rearrange themselves to form sub-grains or cells with low-angle boundaries characterised by <15° misorientation.

Recrystallisation involves the nucleation and growth of relatively defect-free grains within deformed grains, with growth occurring through the movement of high-angle grain-boundaries (>15° misorientation). It is usually the high-angle grain boundaries that are associated with higher internal energy and lower activation energy for mobility than low-angle boundaries during recrystallisation [14]. Full recrystallisation only occurs in the most highly strained regions since dispersoid particles inhibit it in most areas. These particles pin the movement of both dislocation-cell boundaries (low-angle) and grain boundaries (high-angle). Therefore, hot rolled material will not completely recrystallise under normal solution treatment conditions as there is no enough stored internal energy to overcome the pinning effects of the dispersoids. Hot rolled commercial 7xxx series alloys typically comprise a partially recrystallised grain structure, with constituent particles and recrystallised grains distributed along the grain boundaries of un-recrystallised grains, as illustrated in Fig. 2.

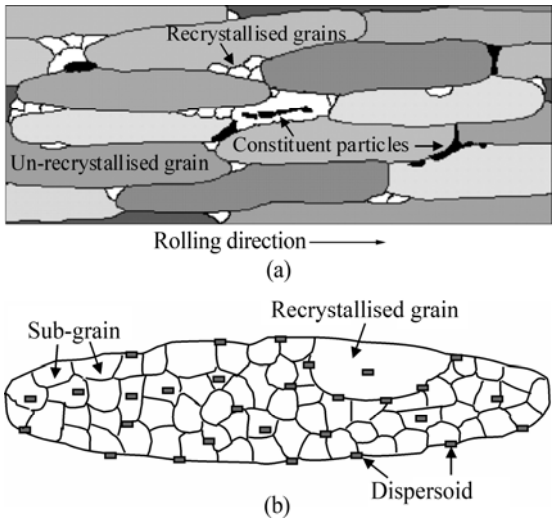

Fig. 2 Schematic illustrations of (a) a typical grain structure after hot rolling and (b) the sub-structure within one partially recrystallised grain (Sub-grains are bounded by dislocation tangles that form low-misorientation boundaries, while recrystallised grains are relatively defect-free and do not exhibit sub-grains. Dispersoids pin grain and sub-grain boundaries.)

2 Materials and methods

This paper is focused on the work that has been carried out mostly at Monash University on a range of important 7xxx series alloys. The composition ranges of some of these alloys are shown in Table 1. Most of the work was associated with 75−80 mm thick plates. Only the AA7020 and some of the AA7075 materials were in the form of extruded products. Since the paper describes aspects from the work of three PhD students and several research fellows at Monash University, it is not possible to describe all the mechanical testing and microstructural characterisation methods in this section. Apart from the specific comments below, the reader is referred to the relevant references throughout the paper.

The quench sensitivity of several 7xxx series alloys was evaluated using a continuous cooling differential scanning calorimetry (DSC) technique developed recently at the University of Rostock [15−18]. Samples were solution treated in a DSC device at 480 °C for 0.5 to 1 h and were then cooled in various DSC devices at a series of linear cooling rates ranging from 0.005 to 3 K/s. Based on a combined evaluation of the DSC data (e.g. plots of excess specific heat capacity vs temperature

Table 1 Composition ranges and upper limits for selected 7xxx series alloys (mass fraction, %)

Alloy	Si	Fe	Cu	Mn	Mg	Cr	Zn	Ti	Zr
AA7020	0.35	0.40	0.20	0.05−0.50	1.0−1.4	0.10−0.35	4.0−5.0	−	0.08−0.20
AA7022	0.50	0.50	0.50−1.0	0.10−0.40	2.6−3.7	0.10−0.30	4.3−5.2	−	−
AA7075	0.40	0.50	1.2−2.0	0.30	2.1−2.9	0.18−0.28	5.1−6.1	0.20	−
AA7079	0.30	0.40	0.40−0.8	0.10−0.30	2.9−3.7	0.10−0.25	3.8−4.8	0.10	−
AA7050	0.12	0.15	2.0−2.6	0.10	1.9−2.6	0.04	5.7−6.7	0.06	0.08−0.15
AA7150	0.12	0.15	1.9−2.5	0.10	2.0−2.7	0.04	5.9−6.9	0.06	0.08−0.15
AA7055	0.10	0.15	2.0−2.6	0.05	1.8−2.3	0.04	7.6−8.4	0.06	0.08−0.25
AA7085	0.06	0.08	1.3−2.0	0.04	1.2−1.8	0.04	7.0−8.0	0.06	0.08−0.15

and precipitation heat vs cooling rate), hardness data and microstructural characterisation of precipitates, novel continuous cooling transformation diagrams were derived initially for alloys AA7020 and AA7150. Cooling rates beyond the limits of conventional DSC devices were achieved using a Bähr DIL 805A/D quenching dilatometer. The DSC/quenching experiments were carried out at the University of Rostock and microstructural characterisation was performed at Monash University.

The retrogression and re-ageing model was developed by Prof. Chris DAVIES and Dr. Adrian GROSVENOR at Monash University. It was based on the precipitation models of MYHR and GRONG [19] and NICOLAS and DESCHAMPS [20]. There are two main concepts. First, the precipitate size distribution is divided into a series of discrete size classes. The stability of each class can then be determined independently, enabling the evolution of the full precipitate size distribution to be tracked. Second, the continuous time-evolution of the particle distribution is divided into a series of small sequential time steps. This removes problems related to changing microstructural, physical and thermodynamic properties. Model inputs include the initial precipitate size distribution and details of the thermal treatment (i.e. temperatures, ramp rates, etc). For each time step, the dissolution or growth of precipitates in each size class is determined by classical equations describing nucleation and growth. Precipitates above the critical size will grow, thereby boosting the next larger size class. After each time step, the remaining solute in solution is recalculated and used for the next time step. Model outputs include the evolving precipitate size distribution, the mean precipitate radius and the precipitate volume fraction. Experimental measurements of these entities may be used to calibrate or verify the model. The model was programmed in MatLab. Full model details and predictions for retrogression and re-ageing of alloy AA7075 were recorded in the PhD thesis of GROSVENOR [21].

3 Results and discussion

Selected results from the homogenisation, solution treatment, quenching and ageing work are presented and discussed under several headings in this section.

3.1 High temperature treatments to dissolve coarse constituent particles

Following hot rolling, AA7150 alloy plates were solution treated at 471−482 °C for up to several hours [22] to dissolve particles that remain from previous processing steps. Dispersoids and Fe-containing particles remain insoluble during solution treatment. Recovery or recrystallisation can occur during solution treatment, depending on the degree of stored strain energy from prior deformation and the effectiveness of the dispersoids in pinning grain boundaries. Since it is desirable from a fracture toughness point of view to minimise the degree of recrystallisation, the solution treatment time and temperature should be kept as low as possible while still achieving the maximum dissolution of soluble particles for the sake of strength and corrosion resistance. These competing effects have been extensively investigated on AA7150 thick plate at Monash University [23−26]. It has been demonstrated that most coarse η precipitates (nominally $MgZn_2$) remaining from previous processing steps can be dissolved in AA7150 alloy within 5 min at 475 °C [26]. This is ascribed to the relatively low solvus temperature of the η-phase and the relatively fast diffusivity of Mg and Zn. For similar reasons, the *T*-phase (nominally $Al_2Mg_3Zn_3$) should also be easy to dissolve. However, *T*-phase was not observed in our AA7150 materials [25].

By contrast, the *S*-phase (nominally Al_2CuMg) is much more difficult to dissolve since its solvus temperature is close to the solution treatment temperature and Cu diffuses more slowly than Mg and Zn. Furthermore, incipient melting temperatures associated with the η and *S* phases in AA7150 have been

determined to be 478 °C and 488 °C, respectively [25,26]. If the material is heated rapidly to these temperatures, then localised melting and property deterioration may occur. However, XU et al [23−26] have demonstrated that such melting can be avoided if the material is heated very gradually. By means of very carefully controlled slow heating and/or step heating, it is possible to increase the solution treatment temperature of AA7150 alloy to slightly over 500 °C without overheating [25,26].

The DSC results in Fig. 3 show endothermic peaks associated with the melting of the η and S phases. In the as-rolled condition, melting peaks associated with both η and S phases are observed (Fig. 3(a)). It is evident from Fig. 3(b) that after solution treating at 475 °C for 8 h, no η-phase remains, but a considerable though smaller amount of S-phase is still present. However, the amount of S-phase decreases with increasing solution treatment temperature until no S-phase remains after the multi-step treatment of (475 °C, 8 h) + (485 °C, 4 h) + (495 °C, 2 h), as illustrated by curves 1−3 in Fig. 3(b). Interestingly, the vertical dashed lines suggest that the melting onset temperature associated with the S-phase, which was measured to be 488 °C after hot rolling, has increased to about 497 °C after solution treating at 475 °C and/or 485 °C. It is therefore possible to increase the solution treatment temperature gradually in small increments until all of the S-phase has dissolved. This is facilitated by both the higher temperature with respect to the S-phase solvus, and the more effective removal of local concentration gradients around dissolving particles (and/or segregation at grain boundaries) due to the increased diffusion rates at these higher temperatures.

The fractographs in Fig. 4 show that a significant amount of rounded S-phase particles are visible on AA7150 tensile fracture surfaces (tested in the short transverse direction after RRA) following a solution treatment of 8 h at 475 °C. By contrast, no S-phase was observed on tensile fracture surfaces after the multi-step treatment of (475 °C, 8 h) + (485 °C, 4 h) + (495 °C, 2 h). Instead, the particles that remain are mainly Al_7Cu_2Fe. The only issue here is that the degree of recrystallisation has increased somewhat after this particular multi-step solution treatment, as shown in the optical micrographs in Fig. 4. Once all of the S-phase has dissolved, there is no more risk of incipient melting around S-phase particles below 500° C. Instead, incipient melting will then start to occur at grain boundaries and triple junctions above 500 °C. These two types of incipient melting were discussed in Ref. [25].

It has been demonstrated that the dissolution of the S-phase by multi-step solution treatment leads to improvements in corrosion, stress corrosion cracking,

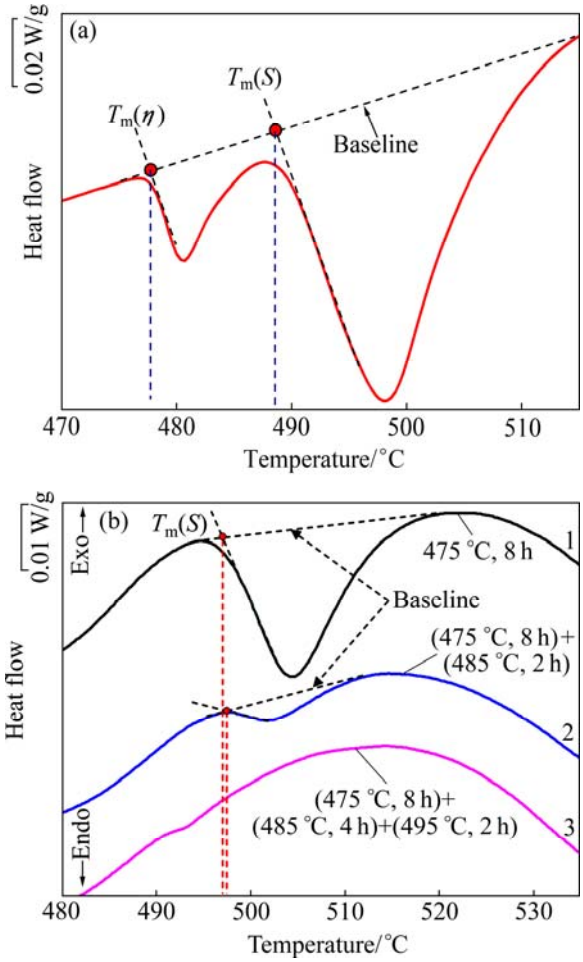

Fig. 3 Partial DSC curves for AA7150 alloy showing incipient melting onset temperatures associated with η and S phases in different conditions: (a) As-rolled condition; (b) After solution treatments (All curves are based on a DSC heating rate of 10 °C/min; curves 1, 2, 3 were measured after RRA, adapted from [25,26])

strength and damage tolerance properties with negligible change in ductility as long as great care is taken to avoid overheating and excessive recrystallisation [23−26]. Some similar findings about property improvements arising from more complete dissolution of soluble coarse constituent particles at elevated solution treatment temperatures have been reported for other 7xxx alloys in China in recent years [27−30].

Attempts have also been made to dissolve the S-phase during the homogenisation treatment. In recent work on DC-cast AA7150 at Monash University, WANG et al [13] found that although the as-cast eutectic starts to melt at around 474 °C, a two-step homogenisation treatment of 40 h at 465 °C followed by 4 h at 480 °C can be used to completely dissolve the η- and S-based constituents. However, the heating rate must be very slow above 455 °C to avoid overheating, since localised melting may occur at relatively low temperatures due to

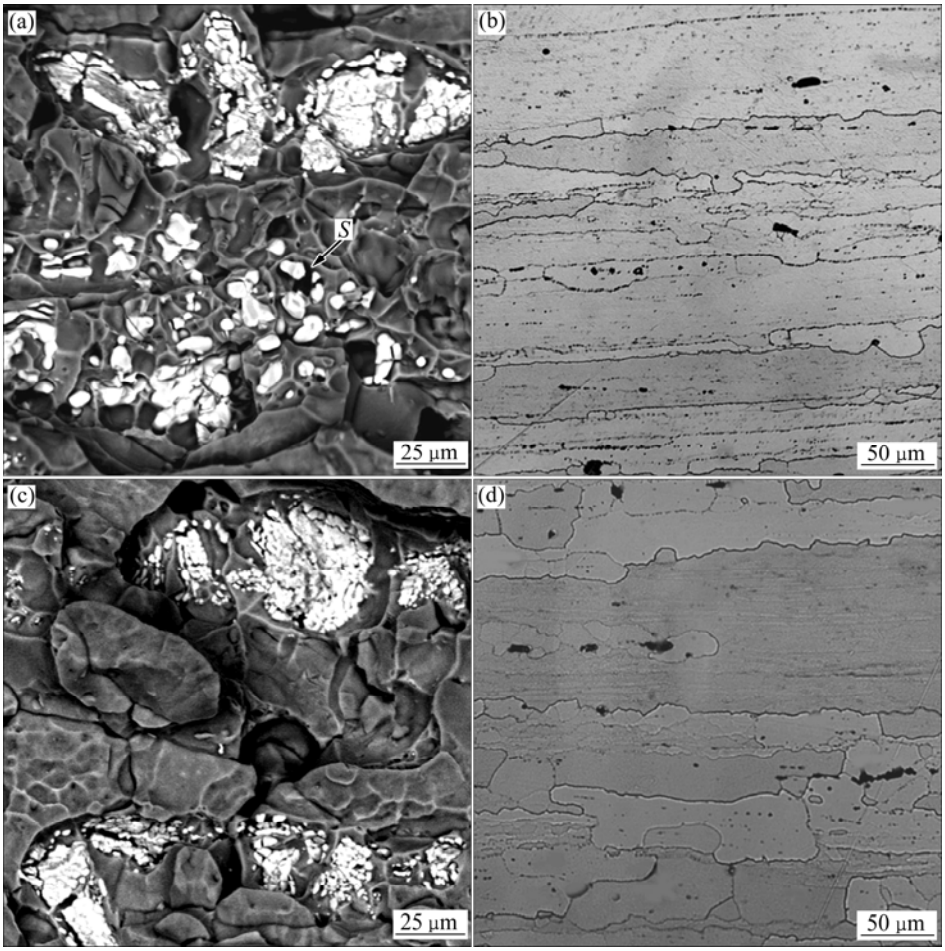

Fig. 4 Backscattered electron SEM images of tensile fracture surfaces and optical micrographs from polished sections corresponding to DSC curves 1 and 3 in Fig. 3: (a, b) Rounded *S* and agglomerated Al_7Cu_2Fe particles; (c, d) Al_7Cu_2Fe particles

the heavily segregated cast microstructure. Another challenge is the fact that η- and *S*-phases may precipitate again during cooling after homogenisation or during subsequent elevated temperature processing. If the post-homogenisation processes are well controlled, at least the particles will not be as coarse as after casting and will therefore be easier to dissolve during solution treatment. Other strategies explored at Monash University to make it easier to dissolve the *S*-phase during solution treatment and thereby improve the overall balance of properties include compositional adjustments to lower the solvus temperature and severe rolling reductions to break up the coarse particles. Some of these options may also be helpful to reducing harmful effects from less soluble coarse intermetallics such as Al_7Cu_2Fe and Mg_2Si. It is well known, for example, that the damage tolerance can be improved by reducing the alloy Fe and Si contents.

Some alternative solution treatments that have been tested are shown in Fig. 1. Multi-step high temperature treatments have been described utilising consecutively increasing temperatures to dissolve more coarse constituents. Another treatment, described in China as a high temperature pre-precipitation (HTPP) treatment, is a multi-step solution treatment utilising consecutively decreasing temperatures to increase the corrosion resistance by means of an improved grain boundary precipitate distribution and chemistry [31,32]. This is similar to the two-step solution treatment patented by the Reynolds Metals Co. [33,34], which was designed to improve the exfoliation corrosion resistance. Unpublished work at Monash University on AA7150 alloy revealed that this Reynolds process with 2-step solution treatment plus 2-step ageing is capable of achieving a higher electrical conductivity and a similar or slightly lower hardness than a standard T7751 process with 1-step solution treatment and 3-step ageing [35]. This is consistent with claims that such a process can improve the corrosion resistance.

3.2 Quench sensitivity and continuous cooling precipitation behaviour

Following solution-treatment, products are rapidly quenched in cold-water to produce a super-saturated

solid solution. Rapid quenching also retains a high concentration of vacancies, which may subsequently facilitate nucleation of the fine-scale strengthening precipitates. Rapid quenching produces significant residual stresses attributable to non-uniform cooling rates through the thickness of the plate and local differences in rates of contraction. Less severe quenching rates are sometimes used to reduce the magnitude of such residual stresses and/or distortion. This may be achieved industrially by reducing the heat transfer rate using methods, such as: 1) quenching into warm water, 2) saturating the quenching water with CO_2 gas, and/or 3) chemically treating the product surface to reduce surface heat transfer [36]. If the quench rate is too high, inter-granular cracking may occur. The risk of such quench cracking occurrence and its severity increase with increasing cooling rate, higher quench temperatures, increasing product size and increasing alloy content [37].

During a slow quench, longer diffusion time may allow coarser precipitates to develop at the grain boundaries, at interfaces with constituent particles, and at dispersoids, thereby reducing the amount of solute available for fine-scale hardening precipitates to form during subsequent ageing [6,38]. If an alloy is susceptible to such precipitation during slow quenching, it is described as being quench sensitive. This is a major issue with thick products, where the quench rates, and therefore the properties, may vary significantly across the thickness of the product. Typically, Zr-containing alloys are less quench sensitive than Cr- or Mn-containing alloys since Al_3Zr dispersoids are more likely to be coherent with the α(Al) matrix and therefore less likely to act as heterogeneous nucleation sites during quenching [39].

Recent work at Monash University on alloy AA7150 has shown that the whole ageing curve after air cooling achieves a clearly higher hardness at the centre of an 80 mm thick plate than on the plate surface. After water quenching, the difference in the ageing curves between surface and centre locations is negligible. This suggests that more solute is lost to non-hardening precipitates during air cooling at plate surface than at plate centre locations, namely the surface is more quench sensitive than the centre. The main microstructural difference between the plate surface and the centre locations is that the surface exhibits a higher degree of recovery and recrystallisation as a result of the more severe rolling deformation on the surface compared with the centre. This results in more heterogeneous nucleation sites such as grain and sub-grain boundaries on the plate surface compared to the plate centre locations. Interestingly, however, SEM and TEM studies at Monash University have shown that metastable coherent $L1_2$ Al_3Zr dispersoids in unrecrystallised grains can transform into incoherent $L1_2$ Al_3Zr dispersoids after recrystallisation. These incoherent $L1_2$ Al_3Zr dispersoids are much more likely to act as heterogeneous nucleation sites than their coherent precursors and are believed to be part of the reason why the plate surface is more quench sensitive than the centre. Some of these findings are illustrated in Fig. 5. Some similar findings have recently been reported for AA7050 sheet in China by ZHANG et al [40].

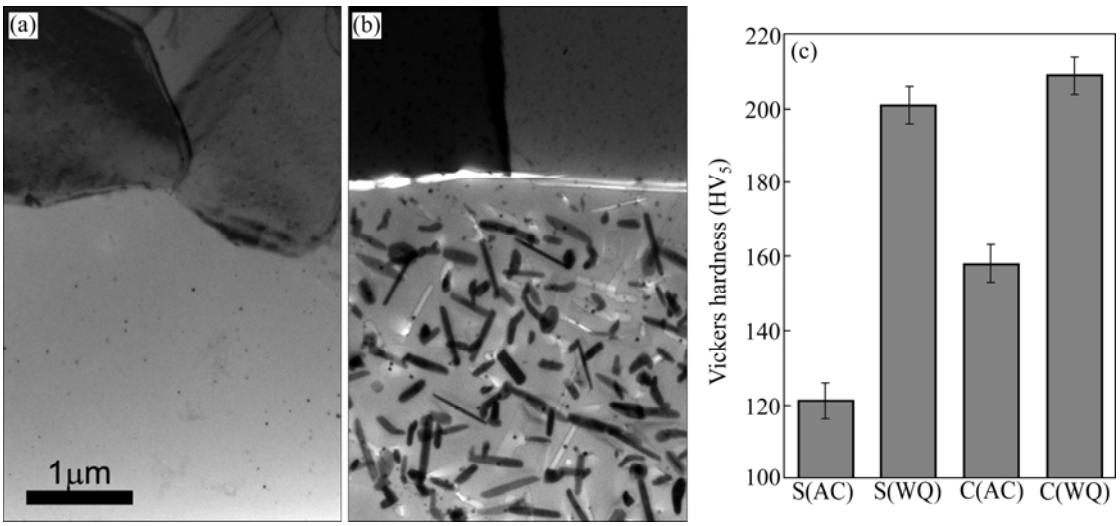

Fig. 5 Bright field TEM images from AA7150 alloy plate centre locations after (a) water quenching and (b) air cooling from a solution treatment temperature of 480 °C. In each case, the lower part of the micrograph shows a fully recrystallised grain, while the upper part shows un-recrystallised sub-grains. The fine dots are $L1_2$ Al_3Zr dispersoids. After air cooling, a large amount of non-hardening precipitates are observed in recrystallized grains but not in un-recrystallised grains. These coarse η-phase precipitates have typically been nucleated on incoherent $L1_2$ Al_3Zr dispersoids. The plot in (c) shows hardness results after 24 h of ageing at 120 °C for both plate surface (S) and centre (C) locations in air cooled (AC) and water quenched (WQ) conditions.

By contrast, studies at Monash University have shown that there is no significant difference in the aged hardness between the samples that were water quenched or air cooled after homogenisation (i.e. without hot rolling). This lack of quench sensitivity before thermo-mechanical processing, but after coherent $L1_2$ Al_3Zr dispersoids have precipitated during homogenisation, further supports the view that recrystallisation during solution treatment can increase the quench sensitivity by making $L1_2$ Al_3Zr dispersoids incoherent with the matrix. Equilibrium $D0_{23}$ Al_3Zr dispersoids have been reported to be incoherent with the matrix and may also increase the quench sensitivity of 7xxx alloys [9,41,42]. However, such equilibrium $D0_{23}$ Al_3Zr dispersoids were not observed in this soon-to-be published work at Monash.

The quench sensitivity of 7xxx series Al alloys has been studied for over 50 years. During this time, many interrupted quenching and isothermal holding studies were carried out to determine time−temperature transformation (TTT) or time−temperature property (TTP) diagrams [43−46]. In recent time, however, there has been a growing interest in studying the more industrially-relevant continuous cooling transformation (CCT) behaviour. Recent studies in China have focused on characterising the continuous cooling behaviour of various 7xxx series alloys by utilising a Jominy end quenching procedure [47,48]. By contrast, recent work in Europe has focused on performing continuous cooling DSC experiments [15−18, 49−51]. The method that was recently developed at the University of Rostock (described in Section 2) was adopted at Monash University because it allows the quench-induced reactions to be quantified. A snapshot of some of the recent results obtained by this method for alloys AA7020 and AA7150 is shown in Figs. 6−8. Full details were given in Ref. [52]. The results in Figs. 6−8 and in Ref. [52] show that the more concentrated alloy AA7150 has higher precipitation heats, higher hardness values and a significantly higher quench sensitivity than alloy AA7020. The continuous cooling precipitation (CCP) diagrams in Fig. 8 show the identities of the various quench-induced precipitation reactions and their locations in continuous cooling temperature−time space. Further microstructural characterisation by electron microscopy and small-angle X-ray scattering is currently underway, as is similar work for several other 7xxx series alloys. One of these is AA7085, which is part of a new generation of high-strength alloys with high Zn/Mg ratio and reduced quench sensitivity [53−55].

3.3 Ageing behaviour and property implications

After solution treatment, quenching and stress relieving, 7xxx series alloys are aged as shown in Fig. 1. Some typical ageing parameters for aerospace plate products are shown in Table 2. Peak strength may be achieved by means of a one-step or two-step ageing treatment. Two-step ageing treatments consist of low temperature ageing followed by higher temperature ageing. Improved combinations of properties may be achieved by more complex treatments such as retrogression and re-ageing (RRA) or interrupted ageing [56]. During ageing, the size and spacing of matrix precipitates increase, with the initial precipitates usually being coherent, and then becoming semi-coherent, and finally incoherent. These changes result in increasing strength associated with an increasing fraction of fine-scale precipitates reaching some optimum distribution at a maximum hardness, followed by decreasing hardness associated with precipitate coarsening that results in a

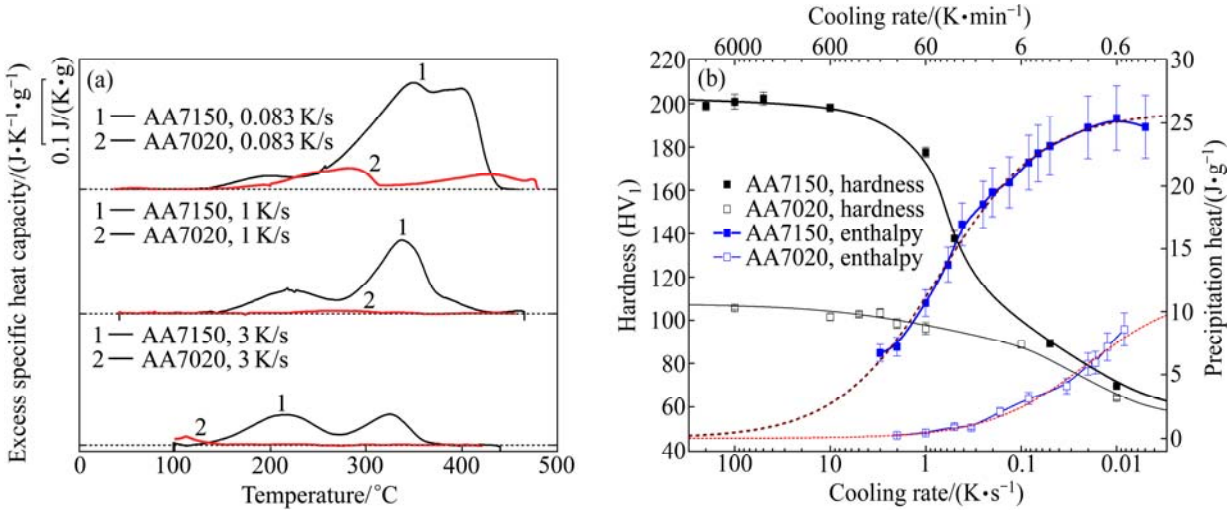

Fig. 6 Continuous cooling DSC results showing (a) three precipitation reactions for AA7150 alloy and at least two precipitation reactions for AA7020 alloy and (b) total precipitation heats (sum of enthalpies for all reactions) and hardness values after ageing at 120 °C for 24 h, as a function of continuous cooling rate; adapted from Ref. [52]

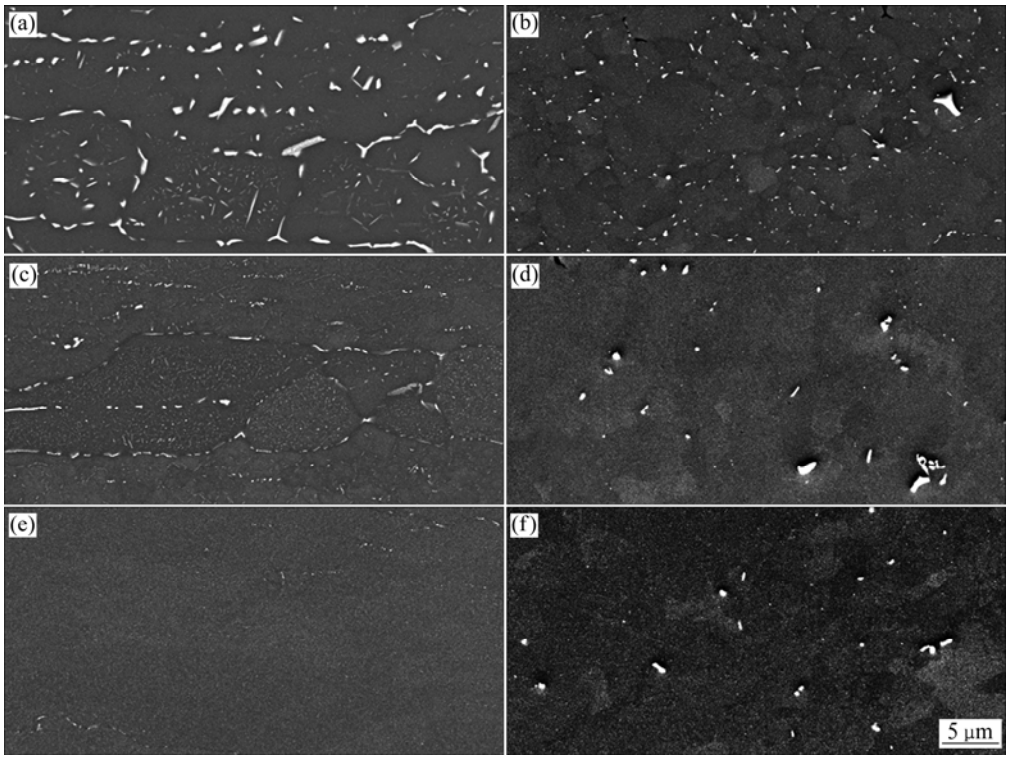

Fig. 7 Backscattered SEM images showing quench-induced precipitates (and some pre-existing intermetallics) in alloys AA7150 and AA7020 at cooling rates of 0.05, 1 and 5 K/s: (a) AA7150, 0.05 K/s; (b) AA7020, 0.05 K/s; (c) AA7150, 1 K/s; (d) AA7020, 1 K/s; (e) AA7150, 5 K/s; (f) AA7020, 5 K/s

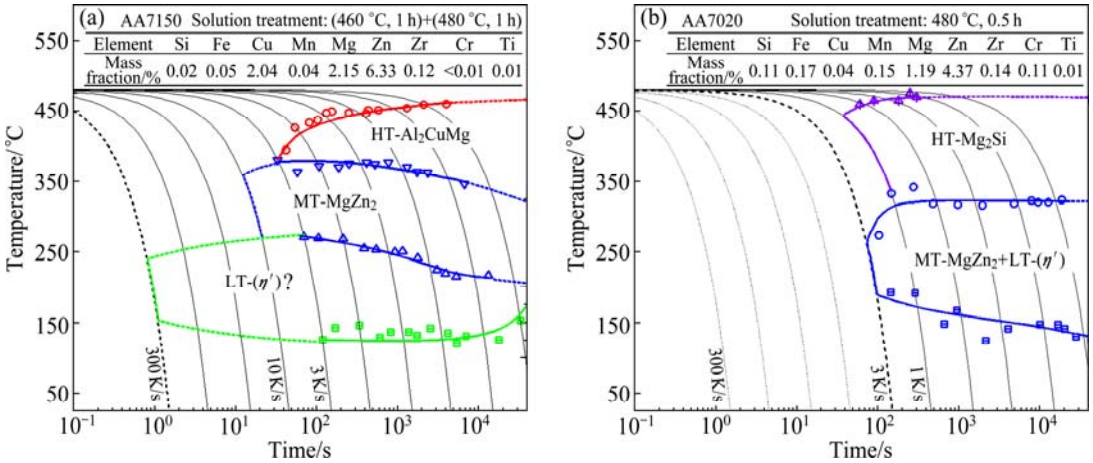

Fig. 8 Continuous cooling precipitation (CCP) diagrams developed for alloys (a) AA7150 and (b) AA7020, showing high temperature (HT), medium temperature (MT) and low temperature (LT) reactions, superimposed over linear cooling rates, adapted from Ref. [52]

Table 2 Typical ageing parameters for selected 7xxx alloy aerospace plate products [22,58]

Alloy	Temper	1st ageing step	2nd ageing step
AA7075	T6	121 °C, 24 h	−
AA7150	T6	121 °C, 24 h	154 °C, 12 h
AA7050	T76	121 °C, 3−6 h	163 °C, 12−15 h
AA7050	T74	121 °C, 3−6 h	163 °C, 24−30 h
AA7050	T73	121 °C, 4−24 h	177 °C, 8−16 h
AA7075	T73	107 °C, 6−8 h	163 °C, 24−30 h

progressive reduction in the number of particles and an increase in average particle spacing. The peak hardness and yield strength for high-strength 7xxx series alloys are typically in the range of VHN 160−200 (450−570 MPa), although higher levels can be achieved.

Precipitates formed at high-angle grain boundaries are usually the equilibrium phase (e.g. η), and are usually much larger than those formed in the matrix (e.g. η'), owing to preferred nucleation and accelerated growth due to faster diffusion of solute along grain boundaries than in the matrix. Grain boundary precipitates drain

solute from adjacent regions so that there is insufficient solute to form matrix precipitates near the grain boundaries. Hence, precipitate-free zones (PFZs) form adjacent to grain boundaries (and around some coarse particles). The formation of PFZs is also influenced by interfaces acting as vacancy sinks, leading to reduced vacancy concentrations and precipitation kinetics around the interfaces.

Early aircraft designs were built with strength-to-weight ratio as the primary design parameter, and hence the peak-aged (T6) heat treatment was first widely adopted for this purpose. The incidence of corrosion-related failures in 7xxx series alloys prompted research into over-aging (T7X) heat-treatments, which were developed in the early 1960s to improve the resistance to stress corrosion cracking (SCC) by means of the T73 temper and resistance to exfoliation corrosion by means of the T76 temper. No SCC service failures have been reported for over-aged AA7075-T73 components [57]. Typically, T73 heat treatments involve a two-stage over-ageing process as shown in Table 2 [22, 58]. Such over-ageing heat treatments reduce the strength by 10%−15% compared with the peak-aged T6 condition. For the tempers shown in Table 2, increasing over-ageing along the sequence T6→T76→T74→T73 progressively decreases the strength but increases the corrosion resistance. Significant weight penalties therefore arise in T73 components designed to carry the same loads as T6 components. Moreover, over-ageing treatments were successful in Al−Zn−Mg−Cu alloys containing >1% Cu, and appeared to be ineffective in some low Cu alloys such as AA7079 for reasons believed to be related to the microchemistry and electrochemical activity of the anodic grain boundary precipitates [59].

In order to improve the SCC resistance of 7xxx series alloys without reducing the strength significantly below T6 values, a three-stage heat treatment known as retrogression and re-ageing (RRA) was developed in the early 1970s [60]. The process originally involved re-treating an already peak-aged alloy at 200−260 °C for 7−120 s, followed by re-ageing the material using the original T6 heat-treatment (e.g. 24 h at 121 °C for AA7075). However, since such times and temperatures do not provide adequate through-heating of thick-sectioned materials, lower retrogression temperatures (180−200 °C) and longer times (45−90 min) were used to make it practical for aircraft components [61]. The RRA process has since been commercially developed as the T77 temper (e.g. AA7150-T7751 and AA7055-T77511) with proprietary ageing parameters, but is widely described as a three-step RRA treatment and is used in the present generation aircraft such as the Boeing 777 [4]. The improvement in corrosion properties for the T77 heat treatment has been attributed to changes in grain boundary precipitate characteristics, such as their microchemistry, electrochemical activity, size and/or distribution [4, 24].

Electrical conductivity and hardness measurements can be used to monitor the precipitation activity during the RRA process, as shown for AA7075 in Fig. 9. The aim of this work at Monash University by KNIGHT [59] was to achieve an electrical conductivity of ~38% IACS (T7 heat-treatment specification) whilst maintaining the hardness higher than 90% of the peak-aged hardness. Broadly speaking, retrogression results in a decrease in hardness and an increase in electrical conductivity as small precipitates are dissolved and large precipitates are coarsened. Such coarsening occurs in a wide range of 7xxx alloys and is illustrated for AA7150 alloy in Fig. 10. Based on the detailed experimental and modelling work at Monash University described in Section 2 (including SAXS to validate the model), GROSVENOR [21] identified three distinct stages of microstructure evolution during the retrogression of alloy AA7075:

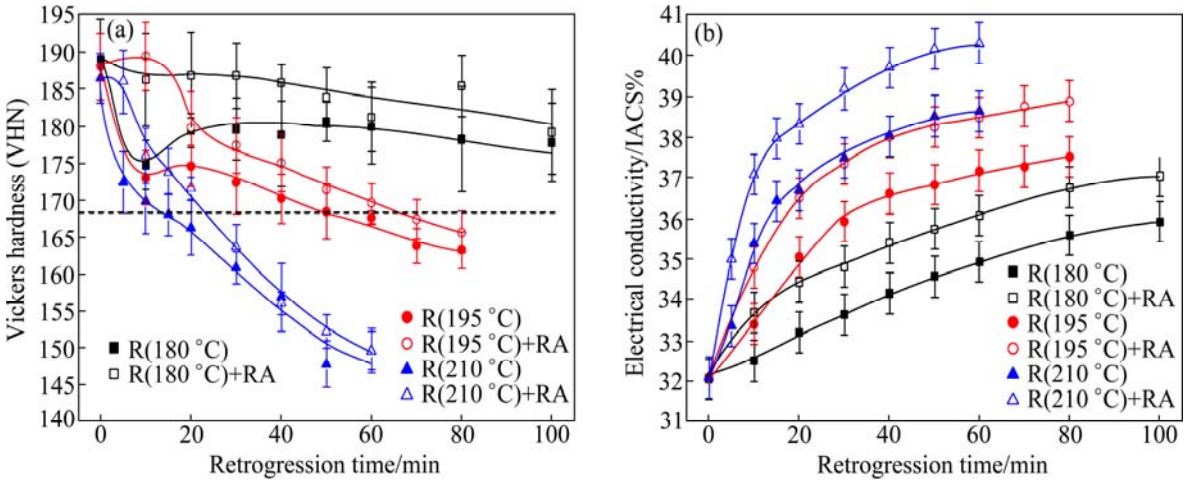

Fig. 9 Effect of retrogression time and temperature (180, 195 and 210 °C) on properties of AA7075: (a) Vickers hardness; (b) Electrical conductivity (The re-aging treatment in this case at 120 °C for 24 h [59])

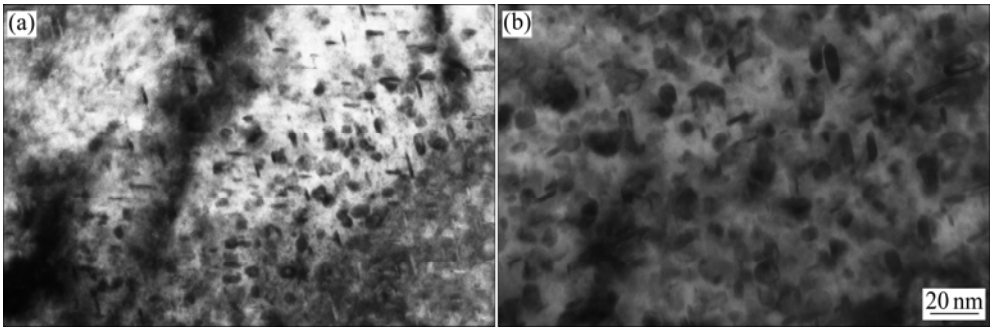

Fig. 10 Typical bright field TEM images for AA7150 alloy after (a) 2.5% stretching + ageing for 24 h at 120 °C and (b) 2.5% stretching + ageing for 24 h at 120 °C + 1.5 h at 185 °C

1) Rapid dissolution of precipitates but similar overall mean precipitate radius during heating to the retrogression temperature.

2) Increases in precipitate volume fraction and mean radius due to the nucleation and growth of precipitates. This coincides with the secondary hardening observed on the R(180 °C) and R(195 °C) curves in Fig. 9(a) between about 10 and 20 min.

3) Precipitate coarsening in the later stages of retrogression. This coincides with the drop in hardness at long retrogression times.

Re-aging, on the other hand, restores some of the hardness due to a re-precipitation of some matrix precipitates and is accompanied by a further increase in electrical conductivity. GROSVENOR [21] identified two distinct stages of microstructure evolution during re-ageing:

1) An increase in the volume fraction of precipitates together with a small increase in mean radius in the early stages of re-ageing. This coincides with the increased strength.

2) A slight coarsening of the precipitates with no observable change in volume fraction at long re-ageing times.

Both this work by GROSVENOR on AA7075 and other work at Monash University by ROMETSCH and XU on AA7150 indicated that there is relatively little change in the microstructure and hardness at re-ageing times between about 12 h and 48 h at 120 °C.

The TEM results in Fig. 11, from work at Monash University on alloy AA7075 [59], showed that over-ageing from a T6 to a T7 temper results in the following microstructural changes:

1) An increase in the matrix precipitate size and spacing;

2) An increase in the grain boundary precipitate size, area fraction and spacing;

3) An increase in the width of the precipitate-free zone.

The same work at Monash University also showed that over-ageing causes a transition from planar type slip to wavy slip. Similar grain boundary microstructures and slip-modes were observed for low-Cu AA7079 and higher-Cu AA7075 for similarly aged T6 or T7 conditions, suggesting that microchemistry may be the cause for different susceptibilities to SCC (up to three orders of magnitude difference in the T7 condition) [59]. Over-ageing was found to increase the SCC resistance (decreased plateau velocities) substantially for slowly quenched AA7079 and AA7022 alloys (with bulk Cu contents of 0.6%−0.9%), contrary to the general view in the literature that over-aging is ineffective for 7xxx series alloys with less than 1% Cu (by mass).

Measurements of the open circuit potential of initially un-corroded brittle intergranular fracture surfaces (produced by fast fracture at −196 °C), and measurements of the changes in potential with time of immersion in aqueous environments, are a novel way of estimating the differences in potential between grain boundary precipitates and adjacent regions. For over-aged alloys, there was an approximately linear relationship between the plateau velocities (on a log scale spanning 4 orders of magnitude) and the potential at the start of corrosion (when the potential was influenced by the large area fraction of up to 30% of grain boundary precipitates) [59,62]. The initial open circuit potential (OCP) and SCC velocity of over-aged alloys appeared to be mainly controlled by the Cu content of the grain boundary precipitates: lower Cu contents result in larger differences in potential between $MgZn_{2-x}Cu_x$ precipitates and adjacent areas, thereby resulting in higher anodic and cathodic reaction rates (and more hydrogen embrittlement).

Increased Cu levels in grain boundary precipitates have also been achieved as a result of high temperature pre-precipitation (HTPP) in both a low-Cu alloy (Al−4.4%Zn−2.4%Mg−0.13%Cu) [32] and a high-Cu AA7055 alloy (Al−8.4%Zn−2.4%Mg−2.6%Cu) [63]. The effects of higher Cu composition were associated

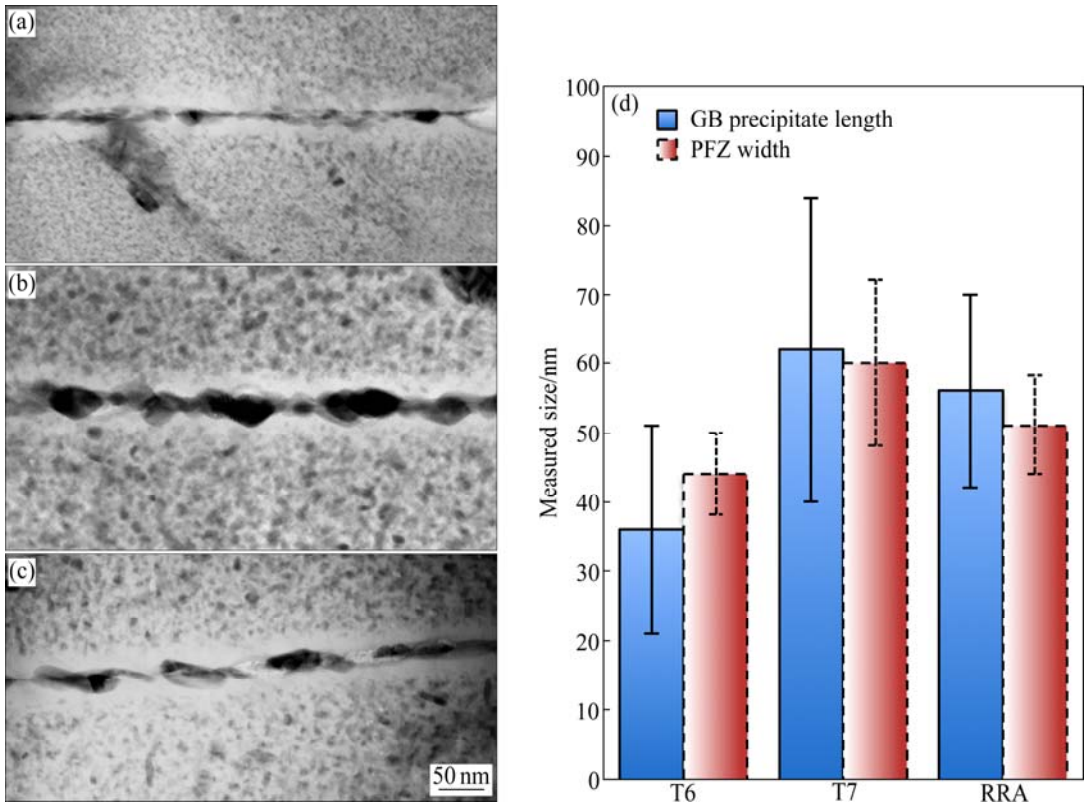

Fig. 11 TEM images (a−c) showing increase in size of matrix and grain boundary precipitates for AA7075 alloy with over-ageing in different conditions: (a) TEM image, T651; (b) TEM image, T7 (T651 + 16 h at 160 °C); (c) TEM image, RRA (T651 + 45 min at 195 °C + 24 h at 120 °C) [59]; (d) Corresponding grain boundary precipitate lengths and PFZ widths

with increased resistance to intergranular corrosion and SCC. XU et al [24] showed that an increased effectively available Cu content from increased *S*-phase dissolution resulted in a higher Cu content in grain boundary precipitates after RRA, which translated into an increased corrosion resistance after RRA. Anomalous small-angle X-ray scattering has been used to show that the Cu substitution for Zn also occurs in the matrix precipitates when an Al−Zn−Mg−Cu alloy is isothermally aged at 160 °C. This result, combined with atom probe tomography that showed the concentrations of Mg and Al in matrix precipitates during the heat treatment to be relatively constant, suggests that the partial substitution was real [64,65].

All the recent work at Monash University supports the view that elevated temperatures (e.g. during over-aging, pre-precipitation or retrogression treatments) activate Cu diffusion, which results in favourable changes in the microchemistry of the grain boundary precipitates and thereby increases the resistance of the alloy to intergranular corrosion and SCC. It is therefore believed that the improved corrosion resistance of the T77 and other T7 tempers is more related to the microchemistry of the grain boundary precipitates than to their size or spacing [59,66].

As mentioned above, heat treatments of 7xxx series alloys can affect the distribution of grain boundary precipitates, PFZ width and matrix precipitate distribution (and slip-mode), which in turn affect the fracture behaviour. When there is a large PFZ and a small area fraction of grain boundary precipitates, significant plastic work is required for voids to grow and impinge on one another during the micro-void coalescence process. However, when there is either a small PFZ width (e.g. peak-aged) or a large area fraction of grain boundary precipitates (e.g. over-aged), voids do not expend much plastic work before growing to a size where they impinge on each other and cause micro-void coalescence. The relative strengths of the PFZ and grain interior determine the extent of strain localisation at grain boundaries and thereby affects the fracture toughness [67]. For this reason it is important to control the quench rate and extent of ageing such that microstructures do not lead to unfavourable properties. Of course, this only applies in the case of ductile intergranular fracture. Other fracture modes (e.g. dimple transgranular) have their own dependency on heat treatment conditions primarily by slip-mode dependence. There are also many other factors that affect the damage tolerance. The improved fracture toughness of 7150-

T7751, for example, has been attributed largely to its un-recrystallised microstructure (giving a more tortuous crack propagation path) and its reduced volume fraction of coarse intermetallic particles [4,68]. As a result, a holistic alloy and process design approach (covering the alloy composition and the whole processing schedule outlined in Fig. 1) is needed if the overall balance of properties is to be improved.

4 Conclusions

This paper has provided an overview of some recent developments in the heat treatment of 7xxx series aluminium alloys that researchers at Monash University have contributed to. The effects of homogenisation, solution treatment, quenching and ageing treatments on the evolution of the microstructure and properties of some important 7xxx series alloys have been discussed. In particular, it has been demonstrated how improvements in the microstructure and properties can be obtained by 1) dissolving unwanted coarse constituent particles such as the *S*-phase through well-controlled high temperature treatments, 2) controlling the quench rate and factors that influence the quench sensitivity, and 3) performing ageing/precipitation treatments at elevated temperatures to increase the Cu content of grain boundary precipitates to render them less anodic with respect to the matrix. Heat treatments 1) and 3) in particular have been found to be very effective in improving the corrosion resistance without decreasing the strength. The quenching work described here demonstrates how the DSC technique recently developed at the University of Rostock may be used to quantify the quench sensitivity by means of continuous cooling precipitation analyses for the purpose of alloy and process design. It must be emphasised that the development of 7xxx series alloys and processing treatments is a complex matter that has been widely studied for over 50 years. If further improvements in microstructures and properties are to be achieved, it is vital that the whole processing route from alloying and casting to final ageing be studied in detail.

Acknowledgements

The authors gratefully acknowledge the following:

The Aluminium Corporation of China Ltd. (Chalco) for supporting aspects of this work financially and providing AA7150 materials as part of the Australia−China International Centre for Light Alloy Research (ICLAR).

Dr. Benjamin MILKEREIT, Prof. Olaf KESSLER and Prof. Christoph SCHICK from the University of Rostock for their significant input in the continuous cooling DSC work.

Prof. Chris DAVIES from Monash University for developing the retrogression and re-ageing Matlab model (as part of the PhD project of Dr Adrian GROSVENOR).

Assoc. Prof. Nick BIRBILIS from Monash University for his expert corrosion input.

Dr. Dao-kui XU and Mr. Sam GAO for their work at Monash University on AA7150 alloy.

The ARC Centre of Excellence for Design in Light Metals and its Directors (first Prof Barry MUDDLE and then Prof Xin-hua WU) for supporting various aspects of this work.

The Monash Centre for Electron Microscopy (MCEM) for providing access to world-class electron microscopy facilities.

References

[1] CHAYONG S, ATKINSON H V, KAPRANOS P. Multistep induction heating regimes for thixoforming 7075 aluminium alloy [J]. Materials Science and Technology, 2004, 20: 490−496.

[2] POLMEAR I J. Light alloys: From traditional alloys to nanocrystals [M]. 4th ed. Oxford: Butterworth-Heinemann, 2006: 421.

[3] LIU Guo-qing, ZHANG Gang, DING Xiang-dong, SUN Jun, CHEN Kang-hua. Dependence of fracture toughness on multiscale second phase particles in high strength Al alloys [J]. Materials Science and Technology, 2003, 19: 887−896.

[4] STARKE E A, STALEY J T. Application of modern aluminum alloys to aircraft [J]. Progress in Aerospace Sciences, 1996, 32: 131−172.

[5] CONSERVA M, Di RUSSO E, CALONI O. Comparison of the influence of chromium and zirconium on the quench sensitivity of Al−Zn−Mg−Cu alloys [J]. Metallurgical Transactions, 1971, 2: 1227−1232.

[6] THOMPSON D S, SUBRAMANYA B S, LEVY S A. Quench rate effects in Al−Zn−Mg−Cu alloys [J]. Metallurgical Transactions, 1971, 2: 1149−1160.

[7] MONDOLFO L F. Aluminum alloys: Structure and properties [M]. London: Butterworths, 1976: 971.

[8] PARK D S, NAM S W. On the characteristics of Mn dispersoid in Al−Zn−Mg alloys [J]. Journal of Materials Science Letters, 1994, 13: 716−718.

[9] ROBSON J D, PRANGNELL P B. Dispersoid precipitation and process modelling in zirconium containing commercial aluminium alloys [J]. Acta Materialia, 2001, 49: 599−613.

[10] ROBSON J D. Optimizing the homogenization of zirconium containing commercial aluminium alloys using a novel process model [J]. Materials Science and Engineering A, 2002, 338: 219−229.

[11] LÜ Xin-yua, GUO Er-jun, ROMETSCH P, WANG Li-juan. Effect of one-step and two-step homogenisation treatments on the distribution of Al_3Zr dispersoids in commercial aluminium alloy 7150 [J]. Transactions of Nonferrous Metals Society of China, 2012, 22: 2645−2651.

[12] ROBSON J D. Microstructural evolution in aluminium alloy 7050 during processing [J]. Materials Science and Engineering A, 2004, 382: 112−121.

[13] WANG L J, XU D K, ROMETSCH P A, GAO S X, ZHANG Y, HE Z B, COUPER M J, MUDDLE B C. Effect of homogenisation parameters on dissolution and precipitation in aluminium alloy AA7150 [J]. Materials Science Forum, 2011, 693: 276−281.

[14] DOHERTY R D, HUGHES D A, HUMPHREYS F J, JONAS J J,

JUUL JENSEN D, KASSNER M E, KING W E, McNELLEY T R, McQUEEN H J, ROLLETT A D. Current issues in recrystallization: A review [J]. Materials Science and Engineering A, 1997, 238: 219−274.

[15] KESSLER O, von BARGEN R, HOFFMANN F, ZOCH H W. Continuous cooling transformation (CCT) diagram of aluminum alloy Al−4.5Zn−1Mg [J]. Materials Science Forum, 2006, 519−521: 1467−1472.

[16] MILKEREIT B, KESSLER O, SCHICK C. Recording of continuous cooling precipitation diagrams of aluminium alloys [J]. Thermochimica Acta, 2009, 492: 73−78.

[17] MILKEREIT B, BECK M, REICH M, KESSLER O, SCHICK C. Precipitation kinetics of an aluminium alloy during Newtonian cooling simulated in a differential scanning calorimeter [J]. Thermochimica Acta, 2011, 522: 86−95.

[18] MILKEREIT B, WANDERKA N, SCHICK C, KESSLER O. Continuous cooling precipitation diagrams of Al−Mg−Si alloys [J]. Materials Science and Engineering A, 2012, 550: 87−96.

[19] MYHR O R, GRONG Ø. Modelling of non-isothermal transformations in alloys containing a particle distribution [J]. Acta Materialia, 2000, 48: 1605−1615.

[20] NICOLAS M, DESCHAMPS A. Characterisation and modelling of precipitate evolution in an Al–Zn–Mg alloy during non-isothermal heat treatments [J]. Acta Materialia, 2003, 51: 6077−6094.

[21] GROSVENOR A. Microstructural evolution during retrogression and reaging treatment of aluminium alloy 7075 [D]. Melbourne: Monash University, 2008: 126−156.

[22] AMS 2772E. Heat treatment of aluminum alloy raw materials [M]. Warrendale, PA: International, 2008: 16−20.

[23] XU D K, BIRBILIS N, LASHANSKY D, ROMETSCH P A, MUDDLE B C. Effect of solution treatment on the corrosion behaviour of aluminium alloy AA7150: Optimisation for corrosion resistance [J]. Corrosion Science, 2011, 53(1): 217−225.

[24] XU D K, BIRBILIS N, ROMETSCH P A. Effect of *S*-phase dissolution on the corrosion and stress corrosion cracking of an as-rolled Al−Zn−Mg−Cu alloy [J]. Corrosion (NACE International, USA), 2012, 68(3): 1−10.

[25] XU D K, BIRBILIS N, ROMETSCH P A. Improved solution treatment for an as-rolled Al–Zn–Mg–Cu alloy: Part I. Characterisation of constituent particles and overheating [J]. Materials Science and Engineering A, 2012, 534: 234−243.

[26] XU D K, BIRBILIS N, ROMETSCH P A. Improved solution treatment for an as-rolled Al–Zn–Mg–Cu alloy: Part II. Microstructure and mechanical properties [J]. Materials Science and Engineering A, 2012, 534: 244−252.

[27] SONG Feng-xuan, ZHANG Xin-ming, LIU Sheng-dan, BAI Tan, HAN Nian-mei, TAN Ji-bo. Effects of solution heat treatment on microstructure and corrosion properties of 7050 Al alloy [J]. Journal of Aeronautical Materials, 2013, 33(4): 14−21. (in Chinese)

[28] CHEN Kang-hua, LIU Hong-wei, ZHANG Zhuo, LI Song, TODD R I. The improvement of constituent dissolution and mechanical properties of 7055 aluminum alloy by stepped heat treatments [J]. Journal of Materials Processing Technology, 2003, 142: 190−196.

[29] CHEN Kang-hua, HUANG Lan-ping. Strengthening-toughening of 7xxx series high strength aluminum alloys by heat treatment [J]. Transactions of Nonferrous Metals Society of China, 2003, 13(3): 484−490.

[30] CHEN Kang-hua, LIU Hong-wei, LIU Yun-zhong. Effect of promotively-solutionizing heat treatment on the mechanical properties and fracture behavior of Al−Zn−Mg−Cu alloys [J]. Acta Metallurgica Sinica, 2001, 37(1): 29−33. (in Chinese)

[31] SONG Min, CHEN Kang-hua. Effects of the enhanced heat treatment on the mechanical properties and stress corrosion behavior of an Al–Zn–Mg alloy [J]. Journal of Materials Science, 2008, 43: 5265−5273.

[32] HUANG Lan-ping, CHEN Kang-hua, LI Song, SONG Min. Influence of high-temperature pre-precipitation on local corrosion behaviors of Al–Zn–Mg alloy [J]. Scripta Materialia, 2007, 56: 305−308.

[33] CANTRELL M A, ANDERSON K R, ARCHIBALD K H. Method of making an AA7000 series aluminum wrought product having a modified solution heat treatment: WO 98/22634 [P]. 1998−05−28.

[34] CANTRELL M A, ANDERSON K R, ARCHIBALD K H. Method of making an AA7000 series aluminum wrought product having a modified solution heat treating process for improved exfoliation corrosion resistance: US5785777 [P]. 1998−07−28.

[35] GAZEAU G, XU D K, ROMETSCH P A. Project on the heat treatment of 7150 alloy [R]. Melbourne: Monash University Internal Student Report, 2009.

[36] CHAKRABARTI D J, LIU J, GOODMAN J H, VENEMA G B, SAWTELL R R, KRIST C M, WESTERLUND R H. Aluminum alloy products having improved property combinations and method of artificially ageing the same: US20020121319 [P]. 2002−09−05.

[37] XU D K, ROMETSCH P A, CHEN H, MUDDLE B C. Influence of solution treatment on microstructure and quench cracking in a water-quenched 7150 aluminium alloy [J]. Materials Science Forum, 2010, 654−656: 934−937.

[38] CONSERVA M, FIORINI P. Interpretation of quench sensitivity in Al−Zn−Mg−Cu alloys [J]. Metallurgical Transactions, 1973, 4: 857−862.

[39] KANNO M, ARAKI I, CUI Q. Precipitation behaviour of 7000 alloys during retrogression and reaging treatment [J]. Materials Science and Technology, 1994, 10: 599603.

[40] ZHANG Xin-ming, LIU Wen-jun, LIU Sheng-dan, ZHOU Ming-zhe. Effect of processing parameters on quench sensitivity of an AA7050 sheet [J]. Materials Science and Engineering A, 2011, 528: 795−802.

[41] SIGLI C. Zirconium solubility in aluminum alloys [J]. Materials Forum, 2004, 28: 1353−1358.

[42] NES E. Precipitation of the metastable cubic Al_3Zr-phase in subperitectic Al−Zr alloys [J]. Acta Materialia, 1972, 20(4): 499−506.

[43] FINK W L, WILLEY L A. Quenching of 75s aluminum alloy [J]. Transactions AIME, 1947, 175: 414−427.

[44] SHUEY R T, TIRYAKIOGLU M, BRAY G H, STALEY J T. Toughness after interrupted quench [J]. Materials Science Forum, 2006, 519−521: 1017−1022.

[45] STALEY J T. Aging kinetics of aluminum alloy 7050 [J]. Metallurgical Transactions, 1973, 5: 929−932.

[46] STALEY J T. Quench factor analysis of aluminium alloys [J]. Materials Science and Technology, 1987, 3: 923−935.

[47] LIU Sheng-dan, LIU Wen-jun, ZHANG Yong. Effect of microstructure on the quench sensitivity of AlZnMgCu alloys [J]. Journal of Alloys and Compounds, 2010, 507: 53−61.

[48] LI Pei-yue, XIONG Bai-qing, ZHANG Yong-an. Quench sensitivity and microstructure character of high strength AA7050 [J]. Transactions of Nonferrous Metals Society of China, 2012, 22: 268−274.

[49] MILKEREIT B, SCHICK C, KESSLER O. Continuous cooling precipitation diagrams depending on the composition of aluminum−magnesium−silicon alloys [C]//12th International Conference on Aluminium Alloys. Yokohama, Japan: The Japan Institute of Light Metals, 2010: 407−417.

[50] ZOHRABYAN D, MILKEREIT B, KESSLER O, SCHICK C. Precipitation enthalpy during cooling of aluminum alloys obtained from calorimetric reheating experiments [J]. Thermochimica Acta, 2012, 529: 51−58.

[51] DESCHAMPS A, TEXIER G, RINGEVAL S, DELFAUT-DURUT L. Influence of cooling rate on the precipitation microstructure in a

medium strength Al−Zn−Mg alloy [J]. Materials Science and Engineering A, 2009, 501: 133−139.
[52] ZHANG Y, MILKEREIT B, KESSLER O, SCHICK C, ROMETSCH P A. Development of continuous cooling precipitation diagrams for aluminium alloys AA7150 and AA7020 [J]. Journal of Alloys and Compounds, 2013, doi: http://dx.doi.org/10.1016/j.jallcom.2013.09.014.
[53] BOSELLI J, CHAKRABARTI D J, SHUEY R T. Metallurgical insights into the improved performance of aluminum alloy 7085 thick products [C]//11th International Conference on Aluminium Alloys. Aachen, Germany: Deutsche Gesellschaft fur Materialkunde e.V. (DGM), 2008: 202−208.
[54] LIU J, KULAK M. A new paradigm in the design of aluminum alloys for aerospace applications [J]. Materials Science Forum, 2000, 331−337: 127−142.
[55] LIU J. Advanced aluminum and hybrid aerostructures for future aircraft [J]. Materials Science Forum, 2006, 519−521: 1233−1238.
[56] LUMLEY R N, POLMEAR I J, MORTON A J. Development of mechanical properties during secondary aging in aluminium alloys [J]. Materials Science and Technology, 2005, 21: 1025−1032.
[57] STALEY J T. History of wrought-aluminum-alloy development [C]// DOHERTY R D. Aluminum alloys contemporary research and applications: Vol. 31. New York: Academic Press, 1989: 3−31.
[58] DAVIS J R. Aluminium and aluminium alloys [M]. Materials Park, OH, USA: ASM International, 1993: 295.
[59] KNIGHT S P. Stress corrosion cracking of Al−Zn−Mg−Cu alloys: Effects of heat-treatment, environment, and alloy composition [D]. Melbourne: Monash University, 2008.
[60] CINA B. Reducing the susceptibility of alloys, particularly aluminium alloys, to stress corrosion cracking: US3856584 [P]. 1974−12−24.
[61] BROWN M H. Three-step aging to obtain high strength and corrosion resistance in Al−Zn−Mg−Cu alloys: US4477292 [P]. 1981.
[62] KNIGHT S P, BIRBILIS N, MUDDLE B C, TRUEMAN A R, LYNCH S P. Correlations between intergranular stress corrosion cracking, grain-boundary microchemistry, and grain-boundary electrochemistry for Al–Zn–Mg–Cu alloys [J]. Corrosion Science, 2010, 52: 4073−4080.
[63] HUANG Lan-ping, CHEN Kang-hua, LI Song. Influence of grain-boundary pre-precipitation and corrosion characteristics of inter-granular phases on corrosion behaviors of an Al–Zn–Mg–Cu alloy [J]. Material Science and Engineering B, 2012, 177: 862−868.
[64] de GEUSER F, DESCHAMPS A. Precipitate characterisation in metallic systems by small-angle X-ray or neutron scattering [J]. Comptes Rendus Physique, 2012, 13: 246−256.
[65] DESCHAMPS A, de GEUSER F. Quantitative characterization of precipitate microstructures in metallic alloys using small-angle scattering [J]. Metallurgical and Materials Transactions A, 2013, 44: 77−86.
[66] XU D K, BIRBILIS N, ROMETSCH P A. The effect of pre-ageing temperature and retrogression heating rate on the strength and corrosion behaviour of AA7150 [J]. Corrosion Science, 2012, 54: 17−25.
[67] VASUDEVAN A K, DOHERTY R D. Grain boundary ductile fracture in precipitation hardened aluminum alloys [J]. Acta Metallurgica, 1987, 35: 1193−1219.
[68] BUCCI R J, WARREN C J, STARKE E A Jr. Need for new materials in aging aircraft structures [J]. Journal of Aircraft, 2000, 37(1): 122−129.

7xxx 系铝合金热处理的进展

Paul A. ROMETSCH, Yong ZHANG, Steven KNIGHT

Department of Materials Engineering, Monash University, Wellington Road, Clayton, VIC 3800, Australia

摘　要：7xxx 系合金是基于 Al−Zn−Mg(−Cu)系的可热处理的锻铝合金，广泛应用于高性能航空结构和运输部件。除了受成分、铸造和形变热处理影响外，材料性能的平衡明显受到其所经历的热处理方式的影响。描述了均匀化、固溶处理、淬火、时效对 7xxx 系高强合金组织和性能的影响。总结了在 Monash 大学进行的有关厚板产品的生产工艺，包括从均匀化到最终的时效处理，以及通过控制微观组织特征，比如弥散体、粗粒子、精细析出相、晶粒结构和晶界特征，来实现组织与性能的平衡。重点陈述了相关方法，如通过高温热处理溶解不需要的粗粒子、基于连续冷却析出行为的淬火敏感性变化、通过实验与建模来研究时效包括一步时效、两步时效、三步时效。对每种情况下的组织与性能都进行研究。

关键词：7xxx 系铝合金；Al−Zn−Mg−Cu；均匀化；固溶处理；淬火；形变与再时效；强度；腐蚀

(Edited by Hua YANG)